Energetic Macroscopic Representation and Inversion-Based Control of a Multi-Level Inverter with Integrated Battery for Electric Vehicles

Clement Mayet, Denis Labrousse, Rihab Bkekri, Francis Roy, Gaël Pongnot

Energetic Macroscopic Representation and Inversion-Based Control of a Multi-Level Inverter with Integrated Battery for Electric Vehicles

Clément MAYET
SATIE – UMR CNRS 8029
Le CNAM – ENS Paris-Saclay
Paris, France
clement.mayet@lecnam.net

Denis LABROUSSE
SATIE – UMR CNRS 8029
Le CNAM – ENS Paris-Saclay
Paris, France
denis.labrousse@satie.ens-cachan.fr

Rihab BKEKRI
SATIE – UMR CNRS 8029
ENS Paris-Saclay
Gif-sur-Yvette, France
rbkekri@satie.ens-cachan.fr

Francis ROY
STELLANTIS
Velizy-Villacoublay, France
francis.roy@stellantis.com

Gaël PONGNOT
SATIE – UMR CNRS 8029
ENS Paris-Saclay
Gif-sur-Yvette, France
gael.pongnot@ens-paris-saclay.fr

***Abstract*—This paper deals with the Energetic Macroscopic Representation (EMR) of a Multi-Level Inverter with Integrated Battery (MLI-IB) for electric vehicles. The MLI-IB consists of modular cascaded modules connected in series. Each module is composed by an individual battery and an H-bridge converter. An inversion-based control is deduced from the EMR to control the output voltage. In addition, the MLI-IB is managed to balance the state-of-charge of the batteries between the various modules.**

Keywords—electric vehicles, integrated battery system, multi-level inverter, simulation and control, battery management system, Energetic Macroscopic Representation.

I. INTRODUCTION

Energy saving, greenhouse gases emissions and fuels depletion are critical issues for the coming decades. The researchers and development activities related to transportation have therefore emphasized the development of high efficiency, clean, and reliable transportation systems [1]. Electric Vehicles (EVs), Hybrid Electric Vehicles (HEVs), and Fuel Cell Electric Vehicles (FCEVs) are expected solutions to increase future mobility while limiting environmental impacts [2]. Nevertheless, the development of EVs faces different challenges such as high initial cost, short driving range (range anxiety) and long charging (refueling) time compared to conventional Internal Combustion Engine Vehicles (ICEVs), which justifies new research and development on these different topics [1], [2].

Focusing on EVs, the traction system is achieved using one or more Electric Machines (EMs), which are supplied by power electronics converters and energy sources. For conventional EVs, a high voltage battery (typically 400 V) is usually considered as main energy source and is a combination of individual battery cells (for example, 3.6 V Li-ion cells) in series and in parallel. However, the reliability of the entire battery depends on the good operating conditions of each cell and requires a Battery Management System (BMS) [3]. The role of the BMS is to passively balance the State-of-Charge (SoC) between the different cells, to manage the thermal aspect of the different cells, and eventually to shut down the system in case of failure [4], [5]. One of the disadvantages of such a topology is that the entire battery pack is limited by the weakest cell in terms of capacity, which can cause the battery to shut down even if the other cells still have energy remaining. Another aspect is related to the necessity to use the technique of Pulse Width Modulation (PWM) to control the inverter and adapt the battery voltage to the supply voltage requested by the EM. This induces switching losses, which mainly depend on the switching frequency, the battery voltage, and the current [6].

The Multi-Level Inverter [7]-[10] with Integrated Battery (MLI-IB) is a potential candidate to solve the aforementioned issues. The MLI-IB integrates battery cells into cascaded H-bridge modules. It aims to fulfill the roles of phase voltage control, BMS, active SoC balancing, and can manage each cell individually [11]. If a cell fails, it can be disconnected from the system, ensuring a continuous operation (albeit in a degraded mode), and improving the reliability of the entire system. The MLI-IB allows removing the passive balancing system of conventional BMS by adding this function directly in the control. In addition, a specific control without PWM technique, which, added to the fact that the voltage of the individual battery used in the MLI-IB is lower than the high voltage of the battery pack used in conventional EVs, leads to drastically reduce the switching losses of power electronics devices. Another advantage of this topology is its modularity. Indeed, this offers opportunities for significant reconfiguration, but also for the recovery and reuse of used battery cells, which is a sustainable way of using them given the current global challenges of energy storage. However, MLI-IB is a more complex system than conventional battery system and must be controlled and assessed for future uses in automotive applications. A first study was carried out to propose a model and control of the MLI-IB, integrating the SoC balancing management [11].

This paper has been achieved within IBIS project, which is funded by ADEME (French Agency for the Ecological Transition) through the Program "Investissement d'Avenir (PIA)".

The objective of this paper is to propose a new organization and control of the MLI-IB based on the Energetic Macroscopic Representation (EMR) methodology. The EMR is a graphical description tool that highlights the energy properties of complex systems while respecting physical causality [12], [13]. Inversion rules have been defined to deduce the Inversion-Based Control (IBC) of the studied system. This methodology makes it possible to better highlight the different functions and levels of control of this new topology. This paper focuses on the MLI-IB. The traction system of the EV is thus outside the scope of this paper. In Section II, the architecture of the MLI-IB is presented. Then, its model, EMR and IBC are developed in Section III. The IBC of the MLI-IB requires defining energy management strategies, which will be explained in Section IV. Finally, the simulation results will be analyzed and discussed in Section V.

II. Architecture of the MLI-IB

The MLI-IB is composed of 3 phases to supply the EM of the EV (Fig. 1). The objective of the MLI-IB is to impose the phase voltage requested by the control of the EM. Each phase *j* consists of *q* modules connected in series. The different modules are controlled to impose their output voltages according to a specific control and strategies which will be presented in the following sections. Each module is composed of an independent battery and two Unit Conversion Elements (UCEs). The battery can be composed by one or several cells in series and/or parallel. The two UCEs form an H-bridge converter which enables bidirectional power flow from each battery. Finally, each UCE is composed by two MOSFETs. The two UCEs are controlled to impose the reference output voltage of the module. This architecture is modular and can be easily reconfigured. It also offers high redundancy, which increases the reliability of the system and gives additional degrees of freedom that can be used in the control especially to add the function of management of the SoC of the battery cells. In the next section, the model, EMR and IBC of one phase of the MLI-IB are presented. Although the traction subsystem is outside the scope of this paper, its model, EMR, and control can be found in [14] as an example.

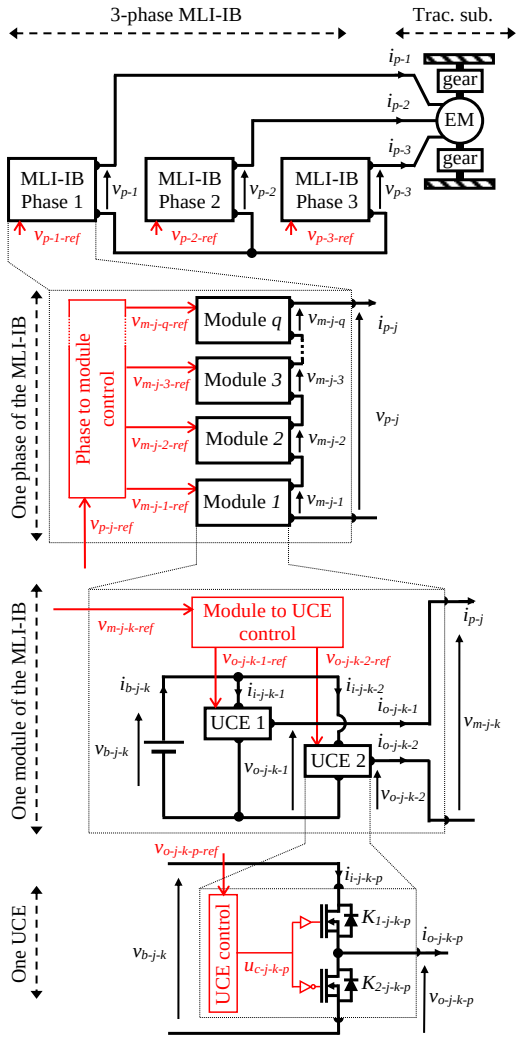

Fig. 1. Traction subsystem of an EV supplied by a 3-phase MLI-IB

III. EMR and IBC of the MLI-IB

This section describes the model of the MLI-IB, which is organized using the EMR. A control structure is then deduced.

A. EMR of the MLI-IB

The EMR is a graphical description tool, which highlight the energy properties of a system [12]. It organizes the system into interconnected basic elements: source of energy (green oval), accumulation of energy (orange crossed rectangle), mono (orange square) or multi (orange circle) domain conversion of energy, and distribution/coupling of energy (double orange square). All elements are connected according to the interaction principle: the product of the action and reaction variables leads to the power exchanged. Furthermore, all the components are described with respect to the physical causality [13].

The EMR of the MLI-IB (Fig. 2) is composed of different elements that convert energy between the batteries (BAT) of the different modules and the EM. This EMR is given for one phase

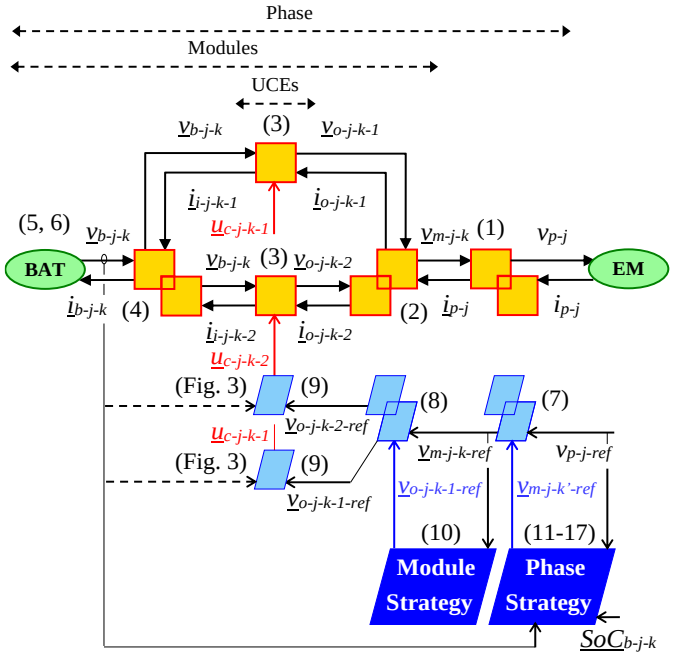

Fig. 2. EMR and IBC of one phase of the MLI-IB.

j and can be duplicated to represent the 3-phase system. The source EM represents one phase of the EM and imposes the phase current $i_{p\text{-}j}$ to the MLI-IB. A coupling element is used to represent the serial connection of the different modules k. A vectorial representation is chosen. The variables $\underline{v}_{m\text{-}j\text{-}k}$ and $\underline{i}_{p\text{-}j}$ are vectors containing respectively the output voltages and currents of the different modules. The phase voltage $v_{p\text{-}j}$ is the sum of all the output voltages $\underline{v}_{m\text{-}j\text{-}k}$ and the currents circulating in the different modules are the common phase current $i_{p\text{-}j}$ (1).

$$\begin{cases} v_{p-j} = \sum_{k=1}^{q} v_{m-j-k} = \sum \underline{v}_{m-j-k} = \sum \begin{bmatrix} v_{m-j-q} \\ \vdots \\ v_{m-j-3} \\ v_{m-j-2} \\ v_{m-j-1} \end{bmatrix} \\ \underline{i}_{p-j-k} = \begin{bmatrix} i_{p-j-q} \\ \vdots \\ i_{p-j-3} \\ i_{p-j-2} \\ i_{p-j-1} \end{bmatrix} = \begin{bmatrix} i_{p-j} \\ \vdots \\ i_{p-j} \\ i_{p-j} \\ i_{p-j} \end{bmatrix} \end{cases} \quad (1)$$

In the following expressions, all variables are 1-by-q vectors, where each component corresponds to a module. Another element is used to represent the coupling between the two UCEs that exist in each module. The output voltages $\underline{v}_{m\text{-}j\text{-}k}$ of the modules are the differences between $\underline{v}_{o\text{-}j\text{-}k\text{-}1}$ and $\underline{v}_{o\text{-}j\text{-}k\text{-}2}$, which are respectively the output voltages of the UCEs 1 and the UCEs 2 (2). The output currents of each UCEs are also given in (2).

$$\begin{cases} \underline{v}_{m-j-k} = \underline{v}_{o-j-k-1} - \underline{v}_{o-j-k-2} \\ \underline{i}_{o-j-k-1} = \underline{i}_{p-j} \\ \underline{i}_{o-j-k-2} = -\underline{i}_{p-j} \end{cases} \quad (2)$$

All the UCEs 1 are represented by a single conversion element. An identical conversion element is used to represent all the UCEs 2. They are described by (3), where p is 1 for the UCEs 1 and 2 for the UCEs 2. The output voltages $\underline{v}_{o\text{-}j\text{-}k\text{-}p}$ depend on the voltages $\underline{v}_{b\text{-}j\text{-}k}$ of the batteries and the control variables $\underline{u}_{c\text{-}j\text{-}k\text{-}p}$ of the UCEs. Equivalent resistances $\underline{R}_{eq\text{-}j\text{-}k\text{-}p}$ are considered to take into account the losses of the UCEs. The input currents $\underline{i}_{i\text{-}j\text{-}k\text{-}p}$ are also expressed in (3).

$$\begin{cases} \underline{v}_{o-j-k-p} = \underline{u}_{c-j-k-p} \times \underline{v}_{b-j-k} \\ \qquad\qquad - \underline{R}_{eq-j-k-p} \times \underline{i}_{o-j-k-p} \\ \underline{i}_{i-j-k-p} = \underline{u}_{c-j-k-p} \times \underline{i}_{o-j-k-p} \end{cases} \quad (3)$$

A last coupling element is used to represent the parallel connection on the battery of the two UCEs of all modules. The voltages $\underline{v}_{b\text{-}j\text{-}k}$ of the batteries are thus common inputs for the UCEs 1 and the UCEs 2 (4). The currents $\underline{i}_{b\text{-}j\text{-}k}$ of the batteries are then the sum of the input currents of the UCEs 1 and of the UCEs 2, as expressed in (4).

$$\begin{cases} \underline{v}_{b-j-k} \ \text{common} \\ \underline{i}_{b-j-k} = \underline{i}_{i-j-k-1} + \underline{i}_{i-j-k-2} \end{cases} \quad (4)$$

Finally, the batteries of each module are represented by a single source, which imposes the voltages $\underline{v}_{b\text{-}j\text{-}k}$ of the different batteries. A simple RE type battery model is used and is described by (5), where $\underline{e}_{b\text{-}j\text{-}k}$ are the open circuit voltages and $\underline{r}_{b\text{-}j\text{-}k}$ are the internal resistances of the batteries. Both parameters depend on the SoCs $\underline{SoC}_{b\text{-}j\text{-}k}$ of the batteries. The SoCs are determined using a Coulomb counting method, which is expressed by (6) and where $\underline{SoC}_{b0\text{-}j\text{-}k}$ is the initial SoCs and $\underline{C}_{b\text{-}j\text{-}k}$ is the effective capacity of the batteries (in Ah).

$$\underline{v}_{b-j-k} = \underline{e}_{b-j-k}\left(\underline{SoC}_{b-j-k}\right) - \underline{r}_{b-j-k}\left(\underline{SoC}_{b-j-k}\right) \times \underline{i}_{b-j-k} \quad (5)$$

$$\underline{SoC}_{b-j-k} = \underline{SoC}_{b0-j-k} - \frac{1}{3600.\underline{C}_{b-j-k}} \int \underline{i}_{b-j-k}.dt \quad (6)$$

B. IBC of the MLI-IB

A local control, which is called IBC, is deduced from the EMR using inversion rules (see the blue part of Fig. 2) [12]. The objective of this control is to impose the output reference phase voltage $v_{p\text{-}j\text{-}ref}$. A tuning path is defined to link the tuning variables $\underline{u}_{c\text{-}j\text{-}k\text{-}1}$ and $\underline{u}_{c\text{-}j\text{-}k\text{-}1}$ to the objective of the control ($v_{p\text{-}j}$). The control structure is obtained by inverting this tuning path step-by-step. Conversion elements are directly inverted and coupling elements require distribution of energy.

The inversion of the coupling element (1) requires sharing the energy between the different modules. Considering it is a coupling of dimension q, it is possible to directly impose the reference output voltages of $q-1$ modules in the vector $\underline{v}_{m\text{-}j\text{-}k'\text{-}ref}$. The reference output voltage of the q^{th} module can be deduced by (7). The vector containing the reference output voltages $\underline{v}_{m\text{-}j\text{-}k\text{-}ref}$ of all the modules is thus obtained by merging the vector $\underline{v}_{m\text{-}j\text{-}k'\text{-}ref}$ and the voltage $v_{m\text{-}j\text{-}q\text{-}ref}$. The vector $\underline{v}_{m\text{-}j\text{-}k'\text{-}ref}$ will be defined in Section IV.B based on a specific voltage generation strategy coupled with a SoC balancing management strategy.

$$v_{m-j-q-ref} = v_{p-j-ref} - \sum \underline{v}_{m-j-k'-ref} \quad (7)$$

The inversion of the second coupling element (2) requires sharing the energy between the UCE 1 and UCE 2 of each module. Considering it is a coupling of dimension 2, it is chosen to directly impose the reference output voltages of the UCEs 1 in the vector $\underline{v}_{o\text{-}j\text{-}k\text{-}1\text{-}ref}$. The reference output voltages of the UCEs 2 are thus defined by (8). The vector $\underline{v}_{o\text{-}j\text{-}k\text{-}1\text{-}ref}$ will be defined in Section IV.A based on the operation strategy of the H-bridge converter, at the module level.

$$\begin{cases} \underline{v}_{o-j-k-1-ref} = \underline{v}_{o-j-k-1-ref} \\ \underline{v}_{o-j-k-2-ref} = \underline{v}_{o-j-k-1-ref} - \underline{v}_{m-j-k-ref} \end{cases} \quad (8)$$

Finally, the conversion elements (3) representing the UCEs are directly inverted. Neglecting the losses, the duty cycles $\underline{\alpha}_{j\text{-}k\text{-}p\text{-}ref}$ of each UCE are defined by (9). They can take any values between 0 and 1 and can be connected to the control variables $\underline{u}_{c\text{-}j\text{-}k\text{-}p}$ in several ways according to the chosen model and control of the UCEs (Fig. 3).

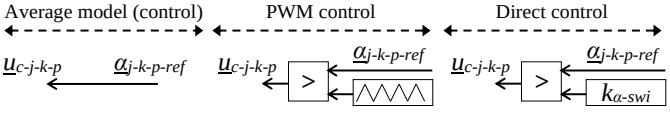

Fig. 3. Inversion of the UCEs.

$$\begin{cases} \underline{\alpha}_{j-k-1-ref} = \dfrac{\underline{v}_{o-j-k-1-ref}}{\underline{v}_{b-j-k}} \\ \underline{\alpha}_{j-k-2-ref} = \dfrac{\underline{v}_{o-j-k-2-ref}}{\underline{v}_{b-j-k}} \end{cases} \quad (9)$$

In case of an average model, the control variables are identical to the duty cycles. However, on the real system, the control variables must be binary signals that can be only 0 or 1. In this case, two different controls are proposed (see Fig. 3). The first is based on PWM technique whereas the second is a direct control where the duty cycles are compared to a constant $k_{a\text{-}swi}$. $k_{a\text{-}swi}$ is a constant between 0 and 1 and corresponds to a threshold that determines the switching condition of the UCEs.

IV. Energy Management Strategies

Based on the defined IBC, two strategies must be defined. First, the operation strategy of the H-bridge converter of each module is defined to distribute the energy between the two UCEs. Then, a specific voltage generation strategy of phase *j*, coupled with a SoC balancing management, is defined to share the energy between the different modules.

A. Operation strategy of an H-bridge converter at the module level

According to the operation strategy of the two UCEs that compose the H-bridge converter of a module (Table I), the reference output voltage $v_{o\text{-}j\text{-}k\text{-}1\text{-}ref}$ of the UCE 1 is used to impose a positive output voltage $v_{m\text{-}j\text{-}k}$ of a module while the reference output voltage $v_{o\text{-}j\text{-}k\text{-}2\text{-}ref}$ of the UCE 2 is kept to zero. On the contrary, the reference output voltage $v_{o\text{-}j\text{-}k\text{-}2\text{-}ref}$ of the UCE 2 is used to impose a negative output voltage $v_{m\text{-}j\text{-}k}$ of a module while the reference output voltage $v_{o\text{-}j\text{-}k\text{-}1\text{-}ref}$ of the UCE 1 is kept to zero. In addition, there are two possibilities for imposing the output voltage $v_{m\text{-}j\text{-}k}$ of a module to zero. In this case, this paper considers that both UCEs impose reference output voltages equal to zero. This operation strategy is described by directly imposing the reference output voltages of the UCEs 1 as defined in (10). As explained previously, in such a case, the reference output voltages of the UCEs 2 are deduced in the IBC by (8).

$$\begin{cases} \underline{v}_{o-j-k-1-ref} = \underline{v}_{m-j-k-ref} & \text{when } \underline{v}_{m-j-k-ref} > 0 \\ \underline{v}_{o-j-k-1-ref} = 0 & \text{when } \underline{v}_{m-j-k-ref} \leq 0 \end{cases} \quad (10)$$

B. Voltage generation strategy at the phase level

As summarized in equation (1), the voltage $v_{p\text{-}j}$ of phase *j* is set by turning on or off some of the modules connected in series. The strategy must activate/deactivate a certain number of modules according to the reference phase voltage $v_{p\text{-}j\text{-}ref}$ and the actual voltages available within each module (i.e. voltages $\underline{v}_{b\text{-}j\text{-}k}$) that can be measured or estimated. There are two possible modes for the voltage generation strategy, namely unipolar and bipolar

TABLE I. Logical Operation of an H-Bridge Converter

Control variables of both UCEs		Output voltages of both UCEs		Output voltage of the module
$u_{c\text{-}j\text{-}k\text{-}1}$	$u_{c\text{-}j\text{-}k\text{-}2}$	$v_{o\text{-}j\text{-}k\text{-}1}$	$v_{o\text{-}j\text{-}k\text{-}2}$	$v_{m\text{-}j\text{-}k}$
0	0	zero	zero	zero
0	1	zero	positive	negative
1	0	positive	zero	positive
1	1	positive	positive	zero

[4], [7]-[10]. The unipolar mode does not allow polarity inversion of any module (i.e. batteries), which means that at any time instant either all batteries of the modules are charging or all are discharging. The bipolar mode allows polarity inversion of some modules, which means that at any time instant it is possible to charge some cells while discharging the others. Only the unipolar mode is considered in this paper. Naturally, this architecture and this strategy involve unbalancing the SoCs of the batteries between the modules. A specific ranking strategy has thus been defined to adapt the order of activation of the different modules accordingly to their actual SoCs [11]. This ranking strategy takes on the role of SoC balancing management and is expressed through an adaptation matrix $\underline{T}(\underline{SoC}_{b\text{-}j\text{-}k})$ (11). This matrix is updated according to a specific period, which must be defined beforehand, or as soon as the maximum delta allowed between the SoCs is reached. The voltage generation strategy uses vectors ranked according to the SoCs of the batteries (variables named $\underline{x}_{xr\text{-}j\text{-}n}$) instead of a natural rank which depends on the topology (variables named $\underline{x}_{x\text{-}j\text{-}k}$) (see Fig. 1).

$$\begin{cases} \underline{x}_{xr-j-n} = \left[\underline{T}\left(\underline{SoC}_{b-j-k}\right)\right] \times \underline{x}_{x-j-k} \\ \underline{x}_{x-j-k} = \left[\underline{T}\left(\underline{SoC}_{b-j-k}\right)\right]^{t} \times \underline{x}_{xr-j-n} \end{cases} \quad (11)$$

The first step of this strategy is thus to rank the voltages of the batteries according to their SoCs (12).

$$\underline{v}_{br-j-n} = \left[\underline{T}\left(\underline{SoC}_{b-j-k}\right)\right] \times \underline{v}_{b-j-k} \quad (12)$$

Then, a simple comparison between the reference phase voltage $v_{p\text{-}j\text{-}ref}$ and a vector, which considers the cumulative sum of the voltages $\underline{v}_{br\text{-}j\text{-}n}$ of the batteries via the function *cumsum* (13), leads to obtain the equivalent control variables at the level of the modules [11]. As the output voltages of the modules can be positive or negative, the sign of the reference output voltage must also be taken into account (14).

$$\underline{u}_{cmr-int-j-n-ref} = v_{p-j-ref} > \text{cumsum}\left(\underline{v}_{br-j-n}\right) \quad (13)$$

$$\underline{u}_{cmr-j-n-ref} = \underline{u}_{cmr-int-j-n-ref} \times \text{sign}\left(v_{p-j-ref}\right) \quad (14)$$

Then, the reference output voltages of the different modules are obtained by a simple product between the vector $\underline{u}_{cmr\text{-}j\text{-}n\text{-}ref}$ and the vector $\underline{v}_{br\text{-}j\text{-}n}$ (15). However, in this way, the last module *n* that could be potentially connected is never considered because the modules are only activated when the summation of their voltages is just below the reference phase voltage as indicated in (13). This leads to always requesting the full battery voltage of a module and never an intermediary voltage. The intermediate reference output voltage of the latter module *n* can be defined as expressed in (16).

$$\underline{v}_{mr-j-n-ref} = \underline{v}_{br-j-n} \times \underline{u}_{cmr-j-n-ref} \quad (15)$$

$$v_{mr-j-n-ref} = v_{p-j-ref} - \sum\left(\underline{v}_{br-j-n} \times \underline{u}_{cmr-j-n-ref}\right) \quad (16)$$

$$\text{only for } \; n = 1 + \sum \underline{u}_{cmr-j-n-ref}$$

At this point, the strategy has defined all the reference output voltages for all modules ranked according to their SoCs. Equation (17) reorganizes the vector according to the natural order (topology) excluding the q^{th} module as explained in (7).

$$\underline{v}_{m-j-k'-ref} = \left[\underline{T}\left(\underline{SoC}_{b-j-k}\right)\right]^{t} \times \underline{v}_{mr-j-n-ref} \quad (17)$$

V. Simulation Results

Simulations are performed to prove the effectiveness of the MLI-IB in controlling the requested phase voltage and balancing the SoC of each battery. The simulated topology consists of 24 modules in series per phase (q = 24). Each module is made up of 4 battery cells (3.6 V Li-ion type) in series and an H-bridge converter. The EM requires a sinusoidal voltage supply with a frequency between 0 and 1 kHz, a voltage amplitude between 0 and 320 V, and an active power up to 58 kW for the 3-phase system. As an example, a complete model of an electric traction system can be found in [14]. However, in this paper the MLI-IB is tested under steady-state conditions and not over a full driving cycle. Therefore, a sinusoidal phase voltage of 200 Hz with an amplitude of 80 V is simulated. The EM imposes a current of amplitude 150 A with a power factor or 0.90 (phase angle of - 0.45 rad), which corresponds to absorbed active and reactive powers of 5.4 kW and 2.6 kVAR, respectively, on each phase.

A. *Results 1: Ability to generate the requested phase voltage*

This subsection presents the ability of the topology and its control to generate an output phase voltage as close as possible to the requested reference voltage. The ideal output voltage is obtained using the average model and control (see Fig. 3). In such a case, the output voltage is strictly equal to its reference as shown on Fig. 4. In this case, seven modules are needed and are sequentially turned on and off to generate the reference output phase voltage. With the average model and control, their output voltages $\underline{v}_{m\text{-}j\text{-}k}$ are identical to their references $\underline{v}_{m\text{-}j\text{-}k\text{-}ref}$. However, the average output voltages of the modules shown on Fig. 4 cannot be directly imposed by the real modules and the control variables must be converted into binary signals. Two different techniques are considered in this paper (see Fig. 3).

The PWM technique allows generating a voltage with high frequency harmonics, which can be filtered if needed. This leads to a voltage waveform for the EM very similar to its reference (Fig. 5). However, this technique also induces high switching losses in the MOSFETs due to the high frequency switching. Another technique using direct control is tested (Fig. 6). In this case the PWM technique is not used, which highly reduces the number of switchings, and thus the losses. The module is activated when its reference voltage reaches a threshold, defined by the coefficient $k_{a\text{-}swi}$ (see Fig. 3). In this case, and depending on its activation, a module can only impose zero or ± the battery voltage as output voltage, which can cause its actual average output voltage to be more or less far from its reference. It means that, depending on the amplitude of the reference phase voltage and the voltage level of the batteries, the quality of the harmonics can highly vary. High phase voltage amplitude with low battery voltages will lead to low harmonics, while low phase voltage amplitude with high battery voltages will lead to high harmonics. Hybrid control, switching between these two techniques, could help reduce switching losses while keeping low harmonics. This aspect needs to be studied further.

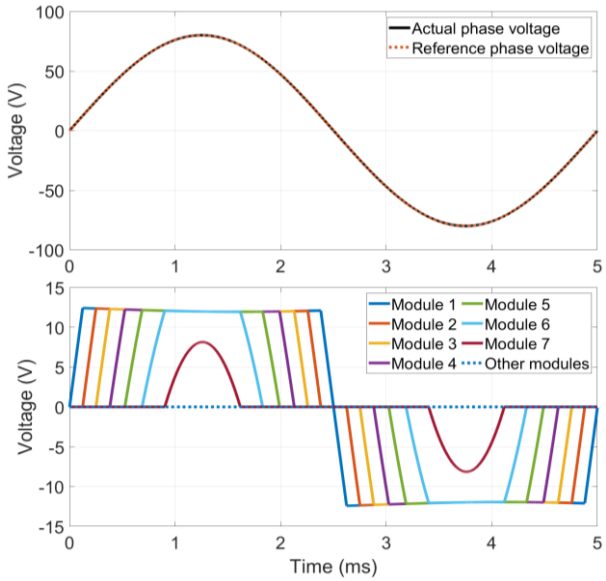

Fig. 4. Simulation results with the ideal average (reference) control.

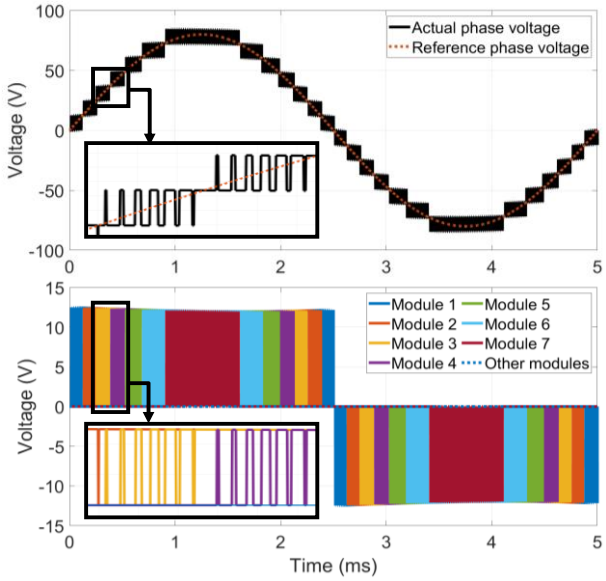

Fig. 5. Simulation results with the PWM control.

B. *Results 2: Ability to balance the SoCs of the different cells*

This subsection presents the ability of the topology and its control to balance the SoCs of the different modules. As explained in Section IV.B, this topology naturally unbalances the SoCs of the different modules. A specific ranking strategy is thus implemented to adapt the order of use of the different modules, and therefore takes the role of battery balancing management strategy [11]. The situation described in subsection V.A is simulated over 1 s with an adaptation of the ranks every 40 ms (Fig. 7). However, this period could be adapted if necessary. The results show that all batteries start with a SoC of 80 %. They are sequentially discharged according to

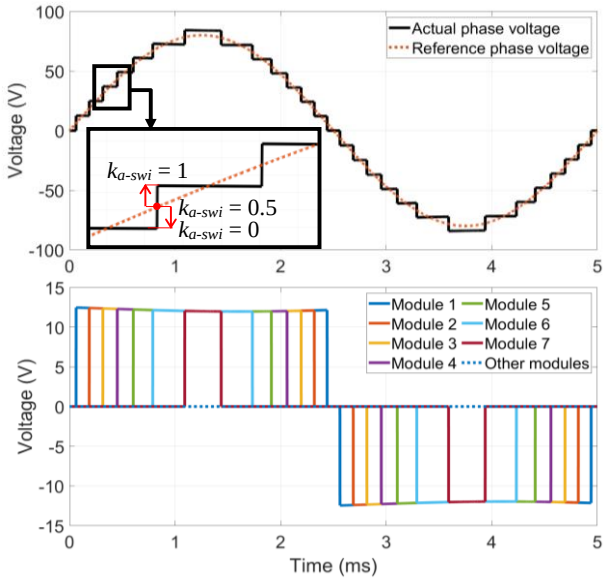

Fig. 6. Simulation results with the direct control.

the activation/deactivation of the different modules. The proposed ranking strategy is able to choose appropriate ranks to maintain an acceptable balance between the different SoCs. In such conditions, all 24 modules are successively used to generate the requested phase voltage although the maximum number of modules activated at the same time is seven as mentioned in the previous subsection. Such a ranking strategy can be adapted according to different conditions. For example, the ranks can be defined according to the sign (charge/discharge) of the instantaneous or of the active power [11]. In addition, the condition for adapting the ranks can be a specific period of time (as in Fig. 7) or a maximum acceptable difference between the SoCs of the modules not to be exceeded. The choice of the ranking conditions has an impact on the losses within the batteries but also on the switching losses of the converters. Future studies will be carried out on this topic.

VI. Conclusion

This paper investigates a Multi-Level Inverter with Integrated-Battery (MLI-IB) for automotive applications. The MLI-IB consists of modular cascaded modules connected in series. Each module is composed of an individual battery and an H-bridge converter. The objective of the MLI-IB is to supply the traction drive of electric vehicles by allowing better management of battery cells compared to a conventional battery system. The MLI-IB is modeled and represented using the Energetic Macroscopic Representation (EMR). Then, an Inversion-Based Control (IBC) is deduced to control and manage the MLI-IB. Preliminary simulation show promising results for future automotive applications. Further work needs to be done to study cell ageing, efficiency, and harmonic generation within such a topology.

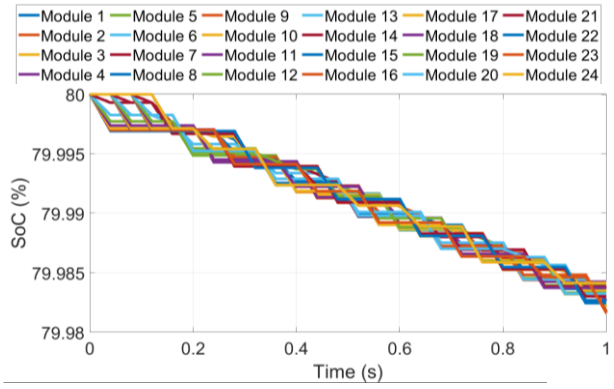

Fig. 7. Simulation results with the ranking strategy (SoCs balancing).

References

[1] M. Eshani, Y. Gao, S. E. Gay, and A. Emadi, "Modern Electric, Hybrid Electric, and Fuel Cell Vehicles: Fundamentals, Theory, and Design," CRC Press, New-York, USA, 2009.

[2] C. C. Chan, "The State of the Art of Electric, Hybrid, and Fuel Cell Vehicles," Proceedings of the IEEE, vol. 95, no. 4, April 2007.

[3] F. H. Gandoman, A. Ahmadi, P. Van den Bossche, J. Van Mierlo, N. Omar, A. E. Nezhad, H. Mavalizadeh, and C. Mayet, "Status and future perspectives of reliability assessment for electric vehiles," Reliability Engineering and System Safety, vol. 183, pp. 1–16, March 2019.

[4] F. Altaf, B. Egardt, and L. J. Mardh, "Load Management of Modular Battery Using Model Predictive Control: Thermal and State-fo-Charge Balancing," IEEE Trans. Control Sys. Technol., vol. 25, no. 1, pp. 47–62, January 2017.

[5] M. A. Hannan, Md. M. Hoque, Y. Yusof, and P. J. Ker, "State-of-the-Art and Energy Management System of Lithium-Ion Batteries in Electric Vehicle Applications: Issues and Recommendations," IEEE Access, vol. 6, pp. 19362–19378, March 2018.

[6] S. Eskandari, K. Peng, B. Tian, and E. Santi, "Accurate Analytical Switching Loss Model for High Voltage SiC MOSFETs Includes Parasitics and Body Diode Rerverse Recovery Effects," IEEE Energy Conversion Congress and Exposition (ECCE), Portland, OR, USA, 23–27 September 2018.

[7] J. Rodriguez, L. G. Franquelo, S. Kouro, J. I. Leon, R. C. Portillo, M. A. M. Prats, and M. A. Pérez, "Multilevel Converters: An Enabling Technology for High-Power Applications," Proc. IEEE, vol. 97, no. 11, pp. 1786–1817, November 2009.

[8] M. Malinowski, K. Gopakumar, J. Rodriguez, and M. A. Pérez, "A survey on Cascaded Multilevel Inverters," IEEE Trans. Ind. Electron., vol. 57, no. 7, pp. 2197–2206, July 2010.

[9] E. Babaei, S. Laali, and Z. Bayat, "A Single-Phase Cascaded Multilevel Inverter Based on a New Basic Unit With Reduced Number of Power Switches," IEEE Trans. Ind. Electron., vol. 62, no. 2, pp. 922–929, February 2015.

[10] R. Vasu, S. K. Chattopadhyay, and C. Chakraborty, "Asymmetric Cascaded H-Bridge Multilevel Inverter With Single DC Source per Phase," IEEE Trans. Ind. Electron., vol. 67, no. 7, pp. 5398–5409, July 2020.

[11] C. Mayet, D. Labrousse, A. Dittrick, B. Revol, R. Bkekri, and F. Roy, "Simulation and Control of a New Integrated Battery System for Automotive Applications," PCIM Europe, Digital Days, Nuremberg, Germany, 3–7 May, 2021, In press.

[12] A. Bouscayrol, J.-P. Hautier, and B. Lemaire-Semail, "Chapter 3: Graphic Formalism for the Control of Multi-Physical Energetic Systems: COG and EMR," in X. Roboam (ed): Systemic design methodologies for electrical energy systems, ISTE Ltd, UK, 2012.

[13] I. Iwasaki, and H. A. Simon, "Causality and model abstraction," Artif. Intell., vol. 67, no. 1, pp. 143–194, 1994.

[14] C. C. Chan, A. Bouscayrol, and K. Chen, "Electric, Hybrid, and Fuel-Cell Vehicles: Architectures and Modeling," IEEE Trans. Veh. Technol., vol. 59, no. 2, pp. 589–598, February 2010.